

Flavoured Lattice Schwinger Model with Chiral Anomaly

Dogukan Bakircioglu

Université Paris-Saclay, INRIA, CNRS, ENS Paris-Saclay, LMF, 91190 Gif-sur-Yvette, France

We introduce the *flavoured lattice Schwinger model*, a (1+1)-dimensional $U(1)$ lattice gauge theory in which the fermion doubling problem is resolved by staggering a \mathbb{Z}_2 flavour degree of freedom rather than staggering chirality. Unlike all standard approaches, the flavoured construction preserves an exact axial $U(1)$ symmetry at finite lattice spacing. We derive the continuum limit, showing the model reduces to two copies of the massless Schwinger model labelled by $\alpha \in \{0, 1\}$. The central result is that the flavoured construction admits a well-defined, regularized, gauge-invariant lattice axial charge Q_G^A with chiral anomaly equation $\langle dQ_G^A/dt \rangle = -(2g/\pi) \int dx \langle E(x) \rangle$ in the continuum limit, derived as a direct dynamical consequence of minimal gauge coupling at finite lattice spacing. Restricting to the $\alpha = 0$ sector recovers the standard single-flavour result. We further show that spatial separation of the flavour sectors can be realised as a helical edge states living on the boundaries of a ribbon shaped (2+1)-dimensional Bernevig–Hughes–Zhang topological insulator. This provides a bulk-boundary picture solution to both the chiral anomaly and fermion doubling.

I. INTRODUCTION

The Schwinger model, quantum electrodynamics (QED) in (1+1)-dimensions, is among the most celebrated exactly solvable models in quantum field theory [1, 2]. Despite its apparent simplicity, it exhibits a rich physical structure: the photon acquires a mass via the Schwinger mechanism, fermions are confined, chiral symmetry is anomalously broken, and the vacuum supports a non-trivial θ -angle structure.

Over the past decade, there has been increasing activity in the study of the lattice Schwinger model using Hamiltonian (real-time) approaches, including tensor-network and related methods [3–12], as well as digital quantum simulation and circuit-based approaches [13–16]. This growing interest is largely driven by recent advances in experimental quantum simulation platforms [17–24].

In contrast, the development of fundamentally new strategies to overcome the notorious *fermion doubling* (FD) problem—appearance of non-physical fermionic modes in lattice theory [25, 26]—has seen comparatively less progress in recent years. In standard lattice formulations, however, exact *onsite* chiral symmetry is either explicitly broken at finite lattice spacing [25–27] or replaced by the Ginsparg–Wilson relation [28–31], and is fully recovered only in the continuum limit. Consequently, a straightforward, gauge-invariant definition of the axial charge at finite lattice spacing is generally lacking. Furthermore, in formulations with explicit breaking, the symmetry is violated directly by the lattice action. This contrasts with the continuum theory, where the classical $U(1)_A$ symmetry is broken strictly anomalously.

This is because all known solutions to the fermion doubling (FD) problem by outright deletion of the

doublers, but due to a global constraint arising from the compactness of the Brillouin zone of the lattice, doublers must carry the opposite chirality relative to the physical solutions [32–35]. Hence, entirely removing the doublers appears to break chiral symmetry. However, the interpretation of doublers as legitimate constituents of the physical chiral symmetry has been shown to be incorrect, since doublers carry the same quantum numbers as their physical counterparts [32–34]. Therefore, doublers should not be counted as part of the chiral symmetry observed in Nature, given that chirally opposite particles can in fact carry different quantum numbers [36–38]. Consequently, if one wishes to claim that lattice regularisation of QFTs is fundamental, a new interpretation of fermion doubling must be provided.

In this work, we apply a new way of fixing FD, introduced in the context of quantum cellular automata (QCA) [39], namely *flavour-staggering-only*. It introduces a \mathbb{Z}_2 flavour degree of freedom that is staggered across lattice sites, we refer to this scheme as *flavoured fermions*. Instead of deleting the doublers, it flavours them. This maps the unphysical solutions into flavoured physical solutions. In contrast with *staggered fermions* [25], continuum physical degrees of freedom are not being staggered, only the flavour degree of freedom is.

Interpreting doublers as new flavours may seem to leave the problem unresolved, since the doublers do still remain. However, the crucial point is that, even though the problem is referred to as fermion doubling, it is not merely about the number of solutions the lattice theory admits. The problem rather lies in the unphysical nature of the doublers, e.g. that high-momentum modes exhibit a low-energy spectrum.

We begin by applying the flavoured fermion strategy in 1 + 1-dimensional Hamiltonian framework, as opposed to its original formulation. The resulting lattice Hamiltonian preserves *both* vector and axial $U(1)$ symmetries

at the lattice level for the two flavours combined, while the continuum limit produces two flavoured copies of the continuum Dirac theory where the symmetries are preserved individually for each flavour.

We systematically study the *flavoured lattice Schwinger model*, obtained by coupling the flavoured fermion lattice to a compact $U(1)$ gauge field. The main results are: (i) we derive the dispersion relation and continuum limit, showing that the model reduces to two copies of the massless Schwinger model labelled by $\alpha \in \{0, 1\}$; (ii) we construct a *gauge-invariant* lattice axial charge Q_G^A and show that it commutes with the hopping Hamiltonian up to $O(a^2)$, so that its non-conservation is a purely dynamical consequence of the electric-field term; (iii) we compute the chiral anomaly and find

$$\left\langle \frac{dQ_G^A}{dt} \right\rangle = -\frac{2g}{\pi} \int dx \langle E(x) \rangle,$$

where the factor of 2 reflects the doubled fermionic content; and (iv) the anomaly coefficient is shown to be independent of the gauge background.

Admittedly, this emergent \mathbb{Z}_2 flavour symmetry is not a fundamental symmetry of the Standard Model, however. Therefore, a mechanism that geometrically separates the two \mathbb{Z}_2 flavour sectors must be provided, such that they are spatially separated.

We show that one way to obtain this physical separation is by considering a 2 + 1-dimensional ribbon shaped topological insulator (TI) [40–44]. Each boundary hosts one flavour in the form of helical edge states, in direct analogy with domain wall fermions, this is a natural geometric realization.

The paper is organised as follows. Section II introduces the lattice Schwinger model and reviews the FD problem and the staggered fermion solution. Section III develops the flavoured fermion construction, its symmetries, and its continuum limit. Section IV embeds the model in a 2+1D TI and derives the helical edge spectrum. Section V presents the main calculation of the chiral anomaly. We conclude in Sec. VII with a discussion of the results. Appendix A contains the detailed derivation of the fermionic correlators entering the anomaly calculation.

II. LATTICE SCHWINGER MODEL

The Hamiltonian of the massless Schwinger model on a lattice with spacing a can be written as [45]

$$H_{\text{sch}} = \sum_{n \in \mathbb{Z}} \frac{i}{2a} \left[(\psi_n^+)^\dagger U_n^\dagger \psi_{n+1}^+ - (\psi_n^-)^\dagger U_n^\dagger \psi_{n+1}^- \right] + \text{h.c.} \\ + \frac{1}{2} g^2 a L_n^2, \quad (1)$$

where $(\psi_n^\pm)^\dagger$ and ψ_n^\pm are fermionic creation and annihilation operators, $U_n = e^{igA_n a}$ is the $U(1)$ parallel transporter with gauge coupling g and one-dimensional gauge field A_n , and L_n is the electric field operator. The operators ψ^+ and ψ^- annihilate left- and right-moving (positive and negative chirality) fermions, respectively. For these operators, we have the following algebras

$$\{\psi_n^\pm, \psi_m^\pm\} = 0, \quad \{(\psi_n^\pm)^\dagger, \psi_m^\pm\} = \delta_{n,m} \delta^{\pm,\pm}, \\ [L_m, U_n] = \delta_{n,m} U_n, \quad [L_m, U_n^\dagger] = -\delta_{n,m} U_n^\dagger. \quad (2)$$

H_{sch} is symmetric under one-site translation $T : \psi_n^\pm \rightarrow \psi_{n+1}^\pm$, and for a constant vector potential $\forall A_n = A$, H_{sch} diagonalizes in the momentum space $p \in [-\pi/a, \pi/a]$, and we find its energy eigenvalues to be

$$E^\pm(p) = \pm \frac{\sin(-pa + gAa)}{a}. \quad (3)$$

Because space is discretised, the momentum space is the *Brillouin zone* (BZ), topologically equivalent to a circle with π/a and $-\pi/a$ identified.

H_{sch} possesses vector and axial $U(1)$ global symmetries, $U_V(1) : \psi_n^\pm \rightarrow e^{i\theta} \psi_n^\pm$ and $U_A(1) : \psi_n^\pm \rightarrow e^{\pm i\theta} \psi_n^\pm$, with conserved charges

$$Q^{V,A} = \sum_{n \in \mathbb{Z}} [(\psi_n^+)^\dagger \psi_n^+ \pm (\psi_n^-)^\dagger \psi_n^-] \quad (4)$$

satisfying

$$[H_{\text{sch}}, Q^V] = [H_{\text{sch}}, Q^A] = 0, \quad (5a)$$

$$[Q^A, Q^V] = 0. \quad (5b)$$

A. Fermion Doubling

We briefly review the fermion doubling (FD) problem, first identified in Refs. [25, 45]; a modern treatment in the QCA framework is given in [39]. The essence of FD is the existence of a degeneracy in the dispersion relation that persists in the continuum limit. We demonstrate it on the lattice Schwinger model in the gauge $\forall A_n = 0$; this corresponds to free lattice fermions in 1+1D [25], and the analysis carries through unchanged.

In the continuum limit $a \rightarrow 0$, around the neighbourhood $\mathcal{U}_0^a = \{p : |p| \ll 1/a\}$, Eq. (3) becomes

$$E_{\text{sch}}^{\pm}(p) \cong \mp p, \quad (6)$$

which is the dispersion relation of the massless Dirac equation in 1+1D. Due to the periodicity of the sine, the same continuum limit also occurs around $\pm\pi/a \mp p$ for $p \ll 1/a$. The union of these points, for $p \ll 1/a$, forms a second open neighbourhood $\mathcal{U}_{\pi}^a = \{\pm\pi/a \mp p : p \ll 1/a\}$. In the exact continuum limit \mathcal{U}_0^a becomes $(-\infty, \infty)$ (finite momenta), which is physical. By contrast, \mathcal{U}_{π}^a contains only infinite-momentum modes and is therefore unphysical; these are the *doublers*. It is important to emphasize that FD does not merely involve an increase in the number of solutions, but rather the emergence of unphysical ones. Consequently, FD represents a qualitative challenge rather than a quantitative one.

In free theory, doublers may be harmless because one can simply restrict to finite-momentum initial states. With interactions ($A_n \neq 0$ for some n), however, doublers can be excited and corrupt the continuum limit. For this reason FD had been taken seriously; solutions fall into two broad categories. The first modifies the Hamiltonian to remove the degeneracy [26, 29]. The second modifies the lattice symmetries to shrink the BZ so that \mathcal{U}_{π}^a is excluded [25, 39, 45].

B. Staggered Fermions

We focus on the second category, and specifically on staggered fermions [25, 28], which solve FD by shrinking the BZ from $[-\pi/a, \pi/a]$ to $[-\pi/2a, \pi/2a]$, thereby excluding \mathcal{U}_{π}^a . This is achieved not by changing the energy eigenvalues but by restricting how lattice sites are assigned to creation and annihilation operators: $\psi_n^+, (\psi_n^+)^\dagger$ are defined only on even sites, while $\psi_n^-, (\psi_n^-)^\dagger$ reside only on odd sites (*staggerisation*). Introducing a single set ϕ_n with $\phi_{2n} = \psi_{2n}^+$ and $\phi_{2n+1} = \psi_{2n+1}^-$, the massless staggered Hamiltonian is

$$H_{\text{stg}} = \sum_{n \in \mathbb{Z}} \frac{i}{2a} (\phi_n)^\dagger (\phi_{n+1} - \phi_{n-1}), \quad (7)$$

or equivalently, in terms of the original chiral fields,

$$H_{\text{stg}} = \sum_{n \text{ even}} \frac{i}{2a} \left[(\psi_n^+)^\dagger (\psi_{n+1}^- - \psi_{n-1}^-) + (\psi_{n+1}^-)^\dagger (\psi_{n+2}^+ - \psi_n^+) \right]. \quad (8)$$

Continuum limit. The continuum limit is taken on the *block lattice* $\tilde{\psi}^+(ka) = (2a)^{-1/2} \phi_{2k}$, $\tilde{\psi}^-(ka) = (2a)^{-1/2} \phi_{2k+1}$. In the block-lattice formalism, H_{stg} reads

$$H_{\text{stg}} = \sum_{n \in \mathbb{Z}} i \left[(\tilde{\psi}^+(na))^\dagger (\tilde{\psi}^-(na) - \tilde{\psi}^-(na-a)) + (\tilde{\psi}^-(na))^\dagger (\tilde{\psi}^+(na+a) - \tilde{\psi}^+(na)) \right]. \quad (9)$$

Defining $x \equiv na$ and applying the Taylor expansion, the continuum limit becomes

$$H_{\text{stg}}^c = \int dx \left[(\tilde{\psi}^+(x))^\dagger (i\partial_x \tilde{\psi}^-(x)) + (\tilde{\psi}^-(x))^\dagger (i\partial_x \tilde{\psi}^+(x)) \right]. \quad (10)$$

Dispersion relation. The staggered theory is invariant under the two-site translation $T^2 : \psi_n^+, \psi_{n+1}^- \rightarrow \psi_{n+2}^+, \psi_{n+3}^-$, giving a BZ $[-\pi/2a, \pi/2a]$ with dispersion relation

$$E_{\text{stg}}^{\pm}(p) = \mp \frac{\sin(pa)}{a}. \quad (11)$$

The continuum limit is taken with block lattice spacing $a' = 2a$:

$$E_{\text{stg}}^{\pm}(p') = \mp \frac{2 \sin(p'a'/2)}{a'}, \quad p' \in [-\pi/a', \pi/a']. \quad (12)$$

As $a' \rightarrow 0$, only the modes in $\mathcal{U}_0^{a'}$ survive — there are no doublers.

Global symmetries. Staggerisation restores neither the axial symmetry on the lattice (chirally opposite operators reside on different sites), nor the lattice axial charge. The only exact lattice symmetry retained is the vector symmetry:

$$[H_{\text{stg}}, Q^V] = 0. \quad (13)$$

The axial symmetry is recovered in the continuum limit through the block-lattice structure, but the absence of a well-defined lattice axial charge makes the study of the chiral anomaly in the staggered formulation indirect [4].

III. FLAVOURED FERMIONS

Flavoured fermions are rooted in staggered fermions but differ in a key respect: instead of staggering the *chirality*, one introduces a \mathbb{Z}_2 *flavour* degree of freedom and staggers that. We define fermionic fields χ^{\pm} and ψ^{\pm} with opposite \mathbb{Z}_2 charges, and assign χ^{\pm} to even sites and ψ^{\pm} to odd sites. The resulting Hamiltonian in the gauge $A_n = 0$ is

$$H_f = \sum_{n \text{ even}} \frac{i}{2a} \left[(\chi_n^+)^\dagger (\psi_{n+1}^+ - \psi_{n-1}^+) - (\chi_n^-)^\dagger (\psi_{n+1}^- - \psi_{n-1}^-) \right] + \text{h.c.} \quad (14)$$

Continuum limit. As for staggered fermions, we introduce a block lattice before taking the continuum limit. Define $\zeta_\circ^\pm(ka) = (2a)^{-1/2}\chi_{2k}^\pm$, $\zeta_\bullet^\pm(ka) = (2a)^{-1/2}\psi_{2k+1}^\pm$, and use the identity

$$\begin{aligned} \zeta^\pm(ka) - \zeta^\pm(ka-a) &= \frac{1}{2}[\zeta^\pm(ka+a) - \zeta^\pm(ka-a)] \\ &\quad - \frac{1}{2}[\zeta^\pm(ka+a) + \zeta^\pm(ka-a) - 2\zeta^\pm(ka)] \end{aligned} \quad (15)$$

where ζ^\pm stands for either ζ_\circ^\pm or ζ_\bullet^\pm . The second bracket on the right-hand side does not contribute to the continuum limit as it produces only terms with $O(a^2)$; we therefore define the *reduced Hamiltonian*

$$\begin{aligned} H_f^R &= \sum_{n \in \mathbb{Z}} \frac{i}{2} \left[(\zeta_\circ^+(na))^\dagger (\zeta_\circ^+(na+a) - \zeta_\circ^+(na-a)) \right. \\ &\quad \left. - (\zeta_\circ^-(na))^\dagger (\zeta_\circ^-(na+a) - \zeta_\circ^-(na-a)) \right] + \text{h.c.}, \end{aligned} \quad (16)$$

for which $\lim_{a \rightarrow 0} H_f = \lim_{a \rightarrow 0} H_f^R$. Diagonalising in the flavour basis with $\tilde{\psi}_\alpha^\pm(na) = 2^{-1/2}[\zeta_\alpha^\pm(na) + (-1)^\alpha \zeta_\bullet^\pm(na)]$ for $\alpha \in \{0,1\}$, the reduced Hamiltonian becomes

$$\begin{aligned} H_f^R &= \sum_{\alpha \in \{0,1\}} (-1)^\alpha \sum_{n \in \mathbb{Z}} \frac{i}{2} \left[(\tilde{\psi}_\alpha^+(na))^\dagger (\tilde{\psi}_\alpha^+(na+a) \right. \\ &\quad \left. - \tilde{\psi}_\alpha^+(na-a)) - (\tilde{\psi}_\alpha^-(na))^\dagger (\tilde{\psi}_\alpha^-(na+a) - \tilde{\psi}_\alpha^-(na-a)) \right]. \end{aligned} \quad (17)$$

In the continuum limit, the flavoured Hamiltonian becomes

$$\begin{aligned} H_f^c &= i \sum_{\alpha \in \{0,1\}} (-1)^\alpha \int dx \left[(\tilde{\psi}_\alpha^+(x))^\dagger \partial_x \tilde{\psi}_\alpha^+(x) \right. \\ &\quad \left. - (\tilde{\psi}_\alpha^-(x))^\dagger \partial_x \tilde{\psi}_\alpha^-(x) \right]. \end{aligned} \quad (18)$$

Note that the \mathbb{Z}_2 flavour symmetry of the discrete theory survives intact in the continuum.

Dispersion relation. H_f is invariant under the two-site translation $T^2 : \chi_n^\pm, \psi_n^\pm \rightarrow \chi_{n+2}^\pm, \psi_{n+2}^\pm$, which induces the BZ $[-\pi/2a, \pi/2a]$. The energy eigenvalues are

$$E_0^\pm(p) = \mp \frac{\sin(pa)}{a}, \quad E_1^\pm(p) = \pm \frac{\sin(pa)}{a}. \quad (19)$$

In the block-lattice continuum limit ($a' = 2a$):

$$E_0^\pm(p') = \mp \frac{2 \sin(p'a'/2)}{a'}, \quad E_1^\pm(p') = \pm \frac{2 \sin(p'a'/2)}{a'}. \quad (20)$$

There are no doublers in either sector. However, the Hilbert space is twice as large as that of the continuum Schwinger model: the $\alpha = 1$ sector, with its opposite-sign dispersion, corresponds precisely to the doubler modes, now promoted to legitimate physical degrees of freedom.

Conserved quantities. H_f possesses both $U_V(1)$ and $U_A(1)$ symmetries: $U_V(1) : \{\chi_n^\pm, \psi_{n+1}^\pm\} \rightarrow \{e^{i\theta} \chi_n^\pm, e^{i\theta} \psi_{n+1}^\pm\}$ and $U_A(1) : \{\chi_n^\pm, \psi_{n+1}^\pm\} \rightarrow \{e^{\pm i\theta} \chi_n^\pm, e^{\pm i\theta} \psi_{n+1}^\pm\}$. The corresponding conserved charges are

$$\begin{aligned} Q_f^{V,A} &= \frac{1}{2} \sum_{n \text{ even}} \left[(\chi_n^+)^\dagger \chi_n^+ \pm (\chi_n^-)^\dagger \chi_n^- \right. \\ &\quad \left. + (\psi_{n+1}^+)^\dagger \psi_{n+1}^+ \pm (\psi_{n+1}^-)^\dagger \psi_{n+1}^- \right], \end{aligned} \quad (21)$$

with $[H_f, Q_f^V] = [H_f, Q_f^A] = 0$ and $[Q_f^A, Q_f^V] = 0$.

The exact lattice $U_A(1)$ symmetry exhibited by H_f should be understood as a symmetry acting on the full flavoured Hilbert space, rather than on a single chiral sector. In particular, while the total axial charge Q_f^A is conserved on the lattice, charges associated with individual flavour sectors are not separately conserved.

We also have the following conserved charges in the continuum,

$$\tilde{Q}_{0,1}^{V,A} = \int dx [(\tilde{\psi}_{0,1}^+)^\dagger \tilde{\psi}_{0,1}^+ \pm (\tilde{\psi}_{0,1}^-)^\dagger \tilde{\psi}_{0,1}^-], \quad (22)$$

and the lattice charges flow to

$$\lim_{a' \rightarrow 0} Q_f^{V,A} = (\tilde{Q}_0^{V,A} + \tilde{Q}_1^{V,A}). \quad (23)$$

As noted in Ref. [2], the expectation values $\langle Q_f^V \rangle$ and $\langle Q_f^A \rangle$ diverge as $a \rightarrow 0$, necessitating regularisation. We introduce the *regularised charges*

$$\begin{aligned} Q_R^{V,A} &= \frac{1}{2} \sum_{n \text{ even}} \left[(\chi_n^+)^\dagger \psi_{n+1}^+ \pm (\chi_n^-)^\dagger \psi_{n+1}^- \right. \\ &\quad \left. + (\psi_{n+1}^+)^\dagger \chi_n^+ \pm (\psi_{n+1}^-)^\dagger \chi_n^- \right], \end{aligned} \quad (24)$$

which flow to

$$\lim_{a' \rightarrow 0} Q_R^{V,A} = (\tilde{Q}_0^{V,A} - \tilde{Q}_1^{V,A}). \quad (25)$$

Even though $\tilde{Q}_0^{V,A} - \tilde{Q}_1^{V,A}$ is conserved in the continuum, $Q_R^{V,A}$ are not conserved on the lattice. This is indeed due to the second order terms that we neglected

at Eq.(15), and we have the following commutation relations,

$$\begin{aligned}
[H_f, Q_R^{V,A}] = & \frac{i}{2a} \sum_{n \text{ even}} (\chi_n^+)^{\dagger} (2\chi_n^+ - \chi_{n-2}^+ - \chi_{n+2}^+) \\
& - (\psi_{n+1}^+)^{\dagger} (2\psi_{n+1}^+ - \psi_{n-1}^+ - \psi_{n+3}^+) \quad (26) \\
& \pm (\chi_n^-)^{\dagger} (2\chi_n^- - \chi_{n-2}^- - \chi_{n+2}^-) \\
& \mp (\psi_{n+1}^-)^{\dagger} (2\psi_{n+1}^- - \psi_{n-1}^- - \psi_{n+3}^-).
\end{aligned}$$

In the continuum limit, these terms cancel, and we obtain $\lim_{a \rightarrow 0} [H_f, Q_R^{V,A}] = 0$.

The no-go theorem. From Eq. (19), the energy eigenvalues of flavour $\alpha = 0$ and $\alpha = 1$ have opposite orientations: while $\tilde{\psi}_0^{\pm}$ carries chiral charge \pm , $\tilde{\psi}_1^{\pm}$ carries a chiral charge \mp . This sign reversal is a direct consequence of the doublers residing at \mathcal{U}_1^a rather than \mathcal{U}_0^a , and reflects a fundamental constraint imposed by the compactness of the Brillouin zone. Specifically, the Atiyah–Singer index theorem [46, 47] states that for the Dirac operator on a compact smooth manifold, the net number of chiral zero modes is a topological invariant, which reduces to the Euler characteristic $\chi(\mathcal{M})$ for the de Rham operator. A closely related argument was given in Ref. [33], where it was concluded that the weak interaction cannot be realised on the lattice, since the weak interaction couples differently to fermions of opposite chirality [48]. However, we stress that the index theorem does *not* forbid chiral asymmetry in general; it only forces a fermion and its doubler to carry opposite chirality. Consequently, in the staggered fermion approach to the doubling problem—where ψ_n^- is identified as the doubler of ψ_n^+ —encoding the weak interaction on the lattice is impossible. By contrast, the flavoured fermion formulation introduces additional degrees of freedom that, in principle, admit a chiral-asymmetric coupling [39]. The price to pay, however, is the emergence of a \mathbb{Z}_2 flavour symmetry in the continuum limit that is absent from the Standard Model. A mechanism must therefore be provided that geometrically distinguishes fermions of opposite \mathbb{Z}_2 flavour, rendering them physically separable without requiring the symmetry to be explicitly broken.

IV. REALISATION AS A TOPOLOGICAL INSULATOR

In this section, we discuss a physical realisation of the emergent \mathbb{Z}_2 symmetry appearing in the continuum limit of the flavoured fermions. We embed the 1 + 1-dimensional flavoured fermion theory into a 2 + 1-dimensional bulk modelled as a quantum spin Hall topological insulator in ribbon geometry, drawing inspiration from the domain wall fermion approach to chiral symmetry on the lattice. We show that the two \mathbb{Z}_2 flavours are naturally realised as helical edge states localised on opposite boundaries of the ribbon, providing a physical mechanism that spatially separates fermions

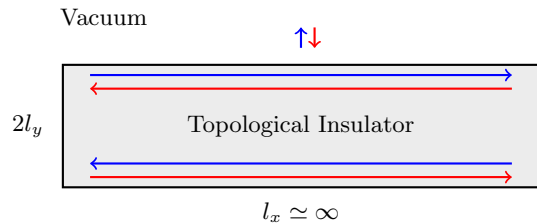


FIG. 1: Ribbon geometry with helical edge states. Arrows along the edges indicate propagation direction, while arrows outside the ribbon denote the associated spin degrees of freedom.

of different flavour and thereby resolves the tension identified at the end of the previous section.

Domain wall fermions We draw some inspiration from another solution of FD, that is called “domain wall fermions” (DWFs) [30, 31]. In this particular solution, they embed the 4D theory into a 5D bulk. For s being the coordinate of the fifth dimension and $2l_5$ being the length, they consider a s dependent mass term $M(s)$ that satisfies $\lim_{s \rightarrow \pm\infty} M(s) = \pm M_0$. The bulk-boundary correspondence dictates that the topological index of the 5D Dirac operator, arising from the transition of the bulk mass, requires the existence of zero mode solutions to the Dirac equation. These modes are exponentially localized at the 4D boundaries (the domain walls). By physically separating the chiral flavours along the fifth dimension, the $U(1)_A$ symmetry is recovered in the $l_5 \rightarrow \infty$ limit, as the overlap between the left-handed mode at $s = -l_5$ and the right-handed mode at $s = l_5$ vanishes, allowing for a lattice realization of chiral fermions that satisfies the Ginsparg-Wilson relation. They avoid the Nielsen-Ninomiya theorem by explicitly breaking the chiral symmetry in the bulk theory and recovering it on the boundary as $l_5 \rightarrow \infty$.

Quantum spin Hall effect. Following the domain wall fermion approach, we embed the flavoured fermion theory into a 2 + 1-dimensional spacetime with spatial geometry of a ribbon: $x \in (-\infty, \infty)$ and $y \in [-l_y, l_y]$. The bulk is modelled as a topological insulator (TI), whose gapped bulk spectrum admits gapless edge states that realise free fermions at low energies [43]. This is precisely the structure required to spatially separate the two flavour sectors: a ribbon-geometry TI supports one edge state on each boundary, with the two edge modes propagating in opposite directions. We restrict to time-reversal-invariant topological insulators, which exhibit the quantum spin Hall effect (QSHE) [41, 42, 49]: at each edge, two counter-propagating modes with opposite spin are present. The ribbon geometry therefore supports four gapless edge modes in total — two at $y = l_y$ and two at $y = -l_y$ — as illustrated in Fig. 1. These are the helical edge states on which the two \mathbb{Z}_2 flavours will be localised.

Our model. Our aim is to construct a Hamiltonian out of the fermionic fields, χ^\pm, ψ^\pm in the bulk and obtain edge states on the different boundaries having different flavours. We want to continue to the use of square lattice with flavours. For this reason, we study a Hamiltonian in 2 + 1D that is similar to the two dimensional Bernevig-Hughes-Zhang (BHZ) model [40–42], where they have a Hamiltonian on a square lattice with orbital degrees of freedom on each lattice point. In BHZ model, there are four degrees of freedom for electrons, they are either at s -orbitals or p -orbitals with spin up and down. Whereas in our case we do not have spin degrees of freedom nor orbitals, instead we have flavour symmetry and chirality, and we map the flavour degree of freedom to be orbital and the chirality to be spin. We have increased the number of spatial dimensions, we again take them to be discretised, and we keep the number of flavours the same. We have two sub-lattices that are covering the square two-dimensional lattice with the new two-dimensional lattice vectors $a_1 = a(\hat{x} + \hat{y})$ and $a_2 = a(\hat{x} - \hat{y})$, for \hat{x} and \hat{y} are the unit vectors, again a is the lattice separation. In the square two-dimensional lattice the coordinates are given by two integers, $a(n\hat{x} + m\hat{y})$, and the sub-lattices are characterised by whether $n + m$ is even or odd. We have the fermionic fields χ^\pm and ψ^\pm occupying the points $n+m$ even and odd respectively. For the matter of representation, we define $\varphi_{n,m}^\pm = (\chi_{n,m}^\pm, \psi_{n,m}^\pm)^T$, and indeed $\psi_{n,m}^\pm = 0, \chi_{n,m}^\pm = 0$ for $n+m$ even and odd respectively. In the bulk we study the following Hamiltonian,

$$H_{2D} = a \sum_{n,m} \begin{pmatrix} h_{n,m}^+ & 0 \\ 0 & h_{n,m}^- \end{pmatrix}, \quad (27)$$

with

$$\begin{aligned} h_{n,m}^\pm = & \frac{iA}{2a} [\pm(\varphi_{n,m}^\pm)^\dagger \sigma_x \varphi_{n+1,m}^\pm - (\varphi_{n,m}^\pm)^\dagger \sigma_y \varphi_{n,m+1}^\pm] \\ & + \frac{1}{2a^2} (\varphi_{n,m}^\pm)^\dagger \sigma_z \left[B(\varphi_{n+1,m+1}^\pm + \varphi_{n-1,m+1}^\pm \right. \\ & \quad \left. + \varphi_{n+1,m-1}^\pm + \varphi_{n-1,m-1}^\pm) \right. \\ & \quad \left. + (2M_0 a^2 - 4B)\varphi_{n,m}^\pm \right] + \text{h.c.}, \end{aligned} \quad (28)$$

where σ_i are the Pauli matrices, A, B, M_0 are the parameters of TI we are considering in the bulk. When the Fourier transform is applied on $\varphi_{n,m}^\pm$, we get $p_x, p_y \in [-\frac{\pi}{a}, \frac{\pi}{a}]$ Fourier variables and since the square lattice is covered by two sublattices, we should have $|p_x + p_y| \leq \frac{\pi}{a}$. Then the Fourier conjugate of h^\pm is written

$$\begin{aligned} \tilde{h}^\pm(p_x, p_y) = & -\frac{A}{a} (\pm \sin(p_x a) \sigma_x + \sin(p_y a) \sigma_y) \\ & + \left(\frac{2B}{a^2} (\cos(p_x a) \cos(p_y a) - 1) + M_0 \right) \sigma_z, \end{aligned} \quad (29)$$

In the continuum limit the bulk energy spectrum becomes

$$E_{2D}^\pm = \pm \sqrt{A^2(p_x^2 + p_y^2) + (M_0 - B(p_x^2 + p_y^2))^2}, \quad (30)$$

in agreement with the standard BHZ spectrum [40, 41].

Topological solitons. In condensed matter language, the vacuum is a trivial insulator with positive mass, while a TI has a negative mass term in part of the parameter space [44]. The existence of edge states requires a sign change of the mass — a topological soliton (domain wall) [50] — at the TI-vacuum interface. For H_{2D} , edge states exist when $M_0 a^2 < 2B$ with $A = 1$ and $B > 0$.

Zero-energy modes. Following Ref. [41], we find the zero-energy solutions of H_{2D} in the continuum. At $p_x = 0$ and $A = 1$, the operator h^\pm reduces to

$$\tilde{h}_y^\pm = (\tilde{\varphi}^\pm)^\dagger (-i\sigma_y \partial_y + \sigma_z (B\partial_y^2 + M_0)) \tilde{\varphi}^\pm, \quad (31)$$

where $\tilde{\varphi}^\pm(x, y) = \lim_{a \rightarrow 0} \varphi_{n,m}^\pm$. Treating $\tilde{\varphi}^\pm$ as a classical field and applying the same ansatz as in Ref. [50], the classical equation of motion gives

$$(\partial_y - \sigma_x (B\partial_y^2 + M_0)) \tilde{\varphi}^\pm(x, y) = 0. \quad (32)$$

Notably, Eq. (32) does not depend on the chirality index \pm , so the two chiralities share the same zero-mode profile. The general solution is

$$\tilde{\varphi}^\pm(x, y) = C_0 e^{\lambda y} \omega_0^\pm(x) + C_1 e^{-\lambda y} \omega_1^\pm(x), \quad (33)$$

where $\sigma_x \omega_{0,1}^\pm = \pm \omega_{0,1}^\pm$ (eigenvectors of σ_x in the flavour basis, analogous to $\tilde{\psi}_{0,1}$ of the continuum flavoured theory), and λ satisfies

$$B\lambda^2 - \lambda + M_0 = 0, \quad \lambda_\pm = \frac{1 \pm \sqrt{1 - 4BM_0}}{2B}. \quad (34)$$

Edge states. For $B > 0$ and $0 < M_0 \leq B$, we have $\text{Re}(\lambda_\pm) \geq 0$. With open boundary conditions $\tilde{\varphi}^\pm(x, \pm l_y) = 0$, the normalised solutions localised at the two boundaries are

$$\tilde{\varphi}_0^\pm(x, y) = C_0^+ (e^{\lambda_+(y-l_y)} - e^{\lambda_-(y-l_y)}) \omega_0^\pm(x), \quad (35a)$$

$$\tilde{\varphi}_1^\pm(x, y) = C_1^+ (e^{-\lambda_+(y+l_y)} - e^{-\lambda_-(y+l_y)}) \omega_1^\pm(x). \quad (35b)$$

$\tilde{\varphi}_0^\pm$ is localised at $y = l_y$ (top edge) and $\tilde{\varphi}_1^\pm$ at $y = -l_y$ (bottom edge). With the normalisation $(\omega_{0,1}^\pm)^\dagger \omega_{0,1}^\pm = 1$ one finds $C_0^+ = C_1^+$ and, in the large- l_y limit,

$$C_0^+ = C_1^+ \simeq \sqrt{\frac{2\lambda_+ \lambda_- (\lambda_+ + \lambda_-)}{(\lambda_+ - \lambda_-)^2}}. \quad (36)$$

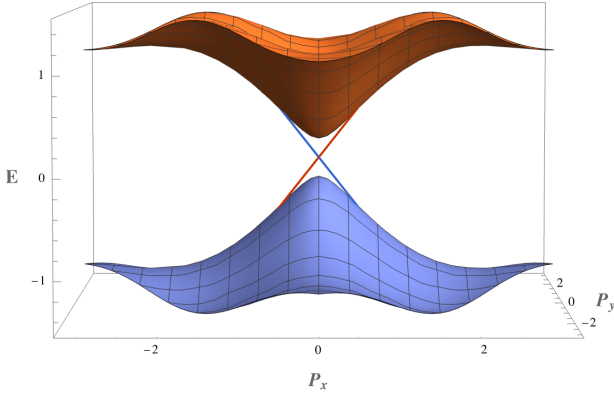


FIG. 2: Bulk energy spectrum of H_{2D} (gapped valence and conduction bands for $a = 1$, $A = 1$, $B = 0.33$, $M_0 = 0.5$) together with the gapless top-edge dispersion. Red and blue lines represent chirality $+$ and $-$, respectively.

Edge Hamiltonians. Integrating the bulk Hamiltonian along the y -axis and using $\sigma_x \omega_{0,1}^\pm = \pm \omega_{0,1}^\pm$, the effective Hamiltonians at the top and bottom edges are

$$\begin{aligned} H_T &= i \int dx [(\omega_0^+)^\dagger \partial_x \omega_0^+ - (\omega_0^-)^\dagger \partial_x \omega_0^-], \\ H_B &= -i \int dx [(\omega_1^+)^\dagger \partial_x \omega_1^+ - (\omega_1^-)^\dagger \partial_x \omega_1^-]. \end{aligned} \quad (37)$$

Both are free Dirac Hamiltonians: the bulk gap is finite, but the edge spectrum is gapless. The bulk and edge dispersions are compared in Fig. 2.

The equations of motion of H_T for ω_0^\pm coincide with those of H_f^c for $\tilde{\psi}_0^\pm$, and those of H_B for ω_1^\pm coincide with those for $\tilde{\psi}_1^\pm$. We may therefore identify $\omega_{0,1}^\pm(x) = \tilde{\psi}_{0,1}^\pm(x)$, giving $H_T + H_B = H_f^c$. This is the key result of this section: the two flavours of the continuum flavoured theory are spatially separated as helical edge states on opposite boundaries of the 2+1D TI. In the broader picture, what we have done is to acknowledge the doublers as legitimate solutions and provide them with a physical domain (the opposite boundary of the TI), rather than discarding or suppressing them. We emphasise that the \mathcal{Z}_2 flavour symmetry is not broken by the topological insulator embedding; rather, it is *geometrically resolved*. The two flavour sectors remain related by \mathcal{Z}_2 in the bulk, but are spatially localised on opposite boundaries, rendering them physically distinguishable and independently accessible.

V. CHIRAL ANOMALY IN THE FLAVOURED LATTICE SCHWINGER MODEL

In this section we couple the flavoured fermions to the $U(1)$ gauge field and study the chiral anomaly. We also

comment on the physical realisation of the anomaly on a single boundary of the TI described in Sec. IV.

Flavoured Schwinger model. When the flavoured fermion solution is applied to H_{sch} , the result is

$$\begin{aligned} H_{\text{sch}}^f &= \sum_{n \text{ even}} \frac{i}{2a} \left[(\chi_n^+)^\dagger (U_n^\dagger \psi_{n+1}^+ - U_{n-1} \psi_{n-1}^+) \right. \\ &\quad \left. - (\chi_n^-)^\dagger (U_n^\dagger \psi_{n+1}^- - U_{n-1} \psi_{n-1}^-) \right] \\ &\quad + \frac{1}{2} g^2 a (L_n^2 + L_{n+1}^2) + \text{h.c.} \end{aligned} \quad (38)$$

We call this the *flavoured lattice Schwinger model*. Its continuum limit is taken using the same block-lattice recipe as in Sec. III. We introduce $\tilde{U}(ka) = U_{2k+1}$, $\tilde{A}(ka) = A_{2k+1}$, and $\tilde{E}(ka) = gL_{2k+1}$ for $k \in \mathbb{Z}$ (inter-block gauge links). Using the generalised block-lattice identity

$$\begin{aligned} &\tilde{U}^\dagger(ka - \frac{a}{2}) \zeta^\pm(ka) - \tilde{U}(ka - a) \zeta^\pm(ka - a) \\ &= \frac{1}{2} [\tilde{U}^\dagger(ka) \zeta^\pm(ka + a) - \tilde{U}(ka - a) \zeta^\pm(ka - a)] \\ &\quad + [\tilde{U}^\dagger(ka - \frac{a}{2}) - 1] \zeta^\pm(ka) + O(a^2), \end{aligned} \quad (39)$$

and performing the flavour diagonalisation of Sec. III, we obtain

$$\begin{aligned} \lim_{a \rightarrow 0} H_{\text{sch}}^f &= i \sum_{\alpha \in \{0,1\}} (-1)^\alpha \int dx \left[(\tilde{\psi}_\alpha^+)^\dagger (\partial_x - ig\tilde{A}) \tilde{\psi}_\alpha^+ \right. \\ &\quad \left. - (\tilde{\psi}_\alpha^-)^\dagger (\partial_x - ig\tilde{A}) \tilde{\psi}_\alpha^- \right] + \frac{1}{2} \int dx \tilde{E}^2(x), \end{aligned} \quad (40)$$

where $\tilde{A}(x) = \lim_{a \rightarrow 0} \tilde{A}(ka)$ and $\tilde{E}(x) = \lim_{a \rightarrow 0} \tilde{E}(ka)$.

Physical content of the continuum limit. The Hamiltonian (40) is a sum of two decoupled, single-flavour Schwinger models. In each copy the Schwinger mechanism generates a bosonic mass [2]

$$m_\alpha^2 = \frac{g^2}{\pi}, \quad \alpha \in \{0,1\}, \quad (41)$$

so the spectrum of the full theory contains two degenerate massive bosonic excitations. Fermion confinement and the θ -angle structure of the vacuum are present in each copy independently. To isolate the physics of a single copy, one restricts to the $\alpha = 0$ sector; in that sector the standard Schwinger result $dQ_0^A/dt = -(g/\pi) \int E dx$ is recovered, while the $\alpha = 1$ sector acts as a spectator. The factor of 2 in the full anomaly equation is therefore a consequence of the doubled spectral content and does not signal an anomaly coefficient that is non-standard for any single species.

Gauge-invariant charges. By arguments analogous to those in Sec. III, H_{sch}^f commutes with the total vector and axial charges $[Q_f^{V,A}, H_{\text{sch}}^f] = 0$. However, as established in Ref. [2], the expectation values $\langle Q_f^{V,A} \rangle$ diverge in the continuum limit. The regularised charges $Q_R^{V,A}$ of Eq. (24) are not gauge-invariant. Their gauge-invariant extension is

$$Q_G^{V,A} = \sum_{n \text{ even}} \left[(\chi_n^+)^{\dagger} U_n^{\dagger} \psi_{n+1}^+ \pm (\chi_n^-)^{\dagger} U_n^{\dagger} \psi_{n+1}^- \right. \\ \left. + (\psi_{n+1}^+)^{\dagger} U_n \chi_n^+ \pm (\psi_{n+1}^-)^{\dagger} U_n \chi_n^- \right]. \quad (42)$$

A remark on uniqueness: Q_G^A is the unique gauge-invariant extension of Q_R^A at $O(a^0)$. Any alternative gauge-invariant bilinear at this order would differ by terms proportional to additional lattice derivatives or longer Wilson lines, which are of $O(a)$ or higher and therefore vanish in the continuum limit without affecting the anomaly coefficient. This uniqueness is important: it means that the factor of 2 in Eq. (47) is not an artifact of a particular operator choice but is intrinsic to the flavoured Hilbert space.

Chiral anomaly. We compute $[H_{\text{sch}}^f, Q_G^{V,A}]$. The hopping part of H_{sch}^f contributes only at $O(a^2)$; at leading order

$$[H_{\text{sch}}^f, Q_G^{V,A}] = \frac{1}{4} g^2 a \sum_{n \text{ even}} [L_n^2, Q_G^{V,A}] + O(a^2). \quad (43)$$

Using the commutation relations (2) and expanding $[L_n^2, Q_G^{V,A}]$, we find

$$[H_{\text{sch}}^f, Q_G^{V,A}] = \frac{1}{2} g^2 a \sum_{n \text{ even}} L_n \\ \times \left[(\psi_{n+1}^+)^{\dagger} U_n \chi_n^+ \pm (\psi_{n+1}^-)^{\dagger} U_n \chi_n^- \right. \\ \left. - (\chi_n^+)^{\dagger} U_n^{\dagger} \psi_{n+1}^+ \mp (\chi_n^-)^{\dagger} U_n^{\dagger} \psi_{n+1}^- \right] + Q_G^{V,A}. \quad (44)$$

We now consider a uniform $U(1)$ background $\forall U_n = e^{igAa}$ on all links, and for this scenario, the expectation value of the gauge-invariant fermionic bilinear is computed in Appendix A:

$$\langle (\psi_{n+1}^{\pm})^{\dagger} U_n \chi_n^{\pm} \rangle = \pm \frac{i}{\pi}. \quad (45)$$

Since $\langle (\psi_{n+1}^{\pm})^{\dagger} U_n \chi_n^{\pm} \rangle$ is pure imaginary, we find $\langle Q_G^{V,A} \rangle = 0$. Inserting Eq. (45) and taking $a \rightarrow 0$:

$$\lim_{a \rightarrow 0} \langle [H_{\text{sch}}^f, Q_G^V] \rangle = 0, \quad (46a)$$

$$\lim_{a \rightarrow 0} \langle [H_{\text{sch}}^f, Q_G^A] \rangle = \frac{2ig}{\pi} \int dx E(x). \quad (46b)$$

Via $d\langle Q_G^A \rangle / dt = i \langle [H_{\text{sch}}^f, Q_G^A] \rangle$, the *lattice chiral anomaly equation* reads

$$\left\langle \frac{dQ_G^A}{dt} \right\rangle = -\frac{2g}{\pi} \int dx \langle E(x) \rangle. \quad (47)$$

Unlike the staggered fermion formulation, where the axial symmetry is explicitly broken by the staggerisation procedure and no well-defined lattice axial charge exists, Q_G^A is a *gauge-invariant, well-defined lattice observable* that commutes with the hopping part of H_{sch}^f up to $O(a^2)$ corrections. Its non-conservation is therefore entirely dynamical and arises purely from the minimal coupling to the gauge field.

The factor of 2 relative to the single-flavour continuum result $dQ^A/dt = (g/\pi) \int E dx$ [2] reflects the doubled fermionic degrees of freedom in the flavoured construction: the \pm chirality sectors each carry an independent contribution to the anomaly, and they add coherently in Q_G^A . The vector charge Q_G^V remains conserved in the continuum limit, consistently with the absence of a vector anomaly. A detailed derivation of the correlator Eq. (45) is given in Appendix A.

Gauge-independence. The correlator $\langle (\psi_{n+1}^{\pm})^{\dagger} U_n \chi_n^{\pm} \rangle$ is computed exactly (Appendix A) and shown to be independent of a uniform background field $U_n = e^{i\theta}$. This gauge-independence is a structural feature of (1+1)D electrodynamics: the gauge field carries no local degrees of freedom and can be removed by a gauge transformation up to global holonomy effects [45, 51]. Hence the gauge-invariant correlator equals its free-theory value $\pm i/\pi$ for any background, and the anomaly coefficient is insensitive to smooth deformations of the gauge field.

VI. CONCLUSION

Summary. We have introduced and systematically studied the flavoured lattice Schwinger model, a (1+1)-dimensional $U(1)$ lattice gauge theory obtained by usage of the flavoured fermion construction [39]. The flavoured construction staggers a \mathbb{Z}_2 flavour degree of freedom across even and odd lattice sites, and thereby preserves *both* the vector and axial $U(1)$ symmetries at the lattice level, in contrast to staggered fermions, which break axial symmetry explicitly. In the continuum limit the theory reduces to two copies of the Schwinger model, labelled by $\alpha \in \{0, 1\}$, with opposite-sign dispersion relations reflecting the reinterpretation of the $\alpha = 1$ sector as the doubler copy.

The central result of this paper is the chiral anomaly equation (47). Unlike in staggered or Wilson formulations, Q_G^A is a finite, well-defined lattice observable whose non-conservation is a direct dynamical consequence of minimal gauge coupling through the electric-field term.

Physical content. The full theory describes two degenerate copies of the Schwinger model in the continuum. Each copy supports a massive bosonic excitation of mass $m^2 = g^2/\pi$, fermion confinement, and a non-trivial θ -angle structure. Restricting to the $\alpha = 0$ sector recovers the standard single-flavour results, while the $\alpha = 1$ copy acts as a spectator whose sole effect on the anomaly is the factor of 2. This separation is physically clean: the two sectors are distinguished by an exactly conserved \mathbb{Z}_2 flavour charge and do not mix at any order in the coupling.

Prospects. The flavoured construction offers a conceptually direct alternative to standard approaches in which chiral symmetry is either explicitly broken or recovered through more involved constructions such as Ginsparg–Wilson fermions: the present model preserves an exact lattice axial symmetry while reproducing the correct anomaly structure dynamically. In particular, the existence of a well-defined, gauge-invariant lattice axial charge Q_G^A enables a direct study of anomaly dynamics without relying on symmetry-breaking regulators or indirect continuum arguments. Several natural extensions present themselves.

Non-Abelian gauge theories. The flavoured fermion construction generalises naturally to $SU(N)$ gauge theories. The chiral anomaly calculation presented here would then yield a non-Abelian chiral anomaly, and the interplay between flavour, colour, and the Nielsen–Ninomiya theorem becomes more intricate.

Quantum simulation. The reinterpretation of doubler

modes as physical flavour degrees of freedom may prove useful in quantum simulation architectures, where additional internal degrees of freedom are naturally available and can be engineered explicitly [18, 20]. In such platforms Q_G^A is a directly measurable observable, making the dynamical generation of the anomaly experimentally

Anomaly inflow and topological insulators. The embedding of the flavoured fermion model into a (2+1)-dimensional Bernevig–Hughes–Zhang topological insulator provides a natural, geometric resolution to the emergent \mathbb{Z}_2 flavour symmetry. By mapping the two flavour sectors to counter-propagating helical edge states, the would be doublers are spatially separated on opposite boundaries of the bulk. Within this bulk-boundary picture, the chiral anomaly observed on the (1+1)-dimensional lattice boundary should be intimately connected to the topological structure of the bulk. An important direction for future work is to explicitly construct the Callan–Harvey anomaly inflow mechanism [52] for the flavoured lattice Schwinger model.

VII. ACKNOWLEDGEMENTS

I would like to thank Pablo Arrighi for his support, insightful suggestions, and assistance in refining the abstract. I am also grateful to Pablo Arnault for his support and his valuable feedback regarding the structure of the manuscript.

-
- [1] J. S. Schwinger, Phys. Rev. **82**, 664 (1951).
 - [2] J. S. Schwinger, Phys. Rev. **128**, 2425 (1962).
 - [3] G. Magnifico, M. Dalmonte, P. Facchi, S. Pascazio, F. V. Pepe, and E. Ercolessi, Quantum **4**, 281 (2020).
 - [4] A. Chatterjee and X.-G. Wen, Phys. Rev. B **107**, 155136 (2023), arXiv:2203.03596 [cond-mat.str-el].
 - [5] R. Dempsey, I. R. Klebanov, S. S. Pufu, and B. Zan, Phys. Rev. Res. **4**, 043133 (2022), arXiv:2206.05308 [hep-th].
 - [6] H. Ohata, “Phase diagram near the quantum critical point in schwinger model at $\theta = \pi$: analogy with quantum ising chain,” (2023), arXiv:2311.04738 [hep-lat].
 - [7] M. C. Bañuls, K. Cichy, J. I. Cirac, and K. Jansen, Journal of High Energy Physics **2013**, 158 (2013).
 - [8] M. C. Bañuls *et al.*, Eur. Phys. J. D **74**, 165 (2020), arXiv:1911.00003.
 - [9] P. Silvi, E. Rico, T. Calarco, and S. Montangero, New Journal of Physics **16**, 103015 (2014).
 - [10] P. Silvi, F. Tschirsich, M. Gerster, J. Jünemann, D. Jaschke, M. Rizzi, and S. Montangero, SciPost Phys. Lect. Notes, **8** (2019).
 - [11] M. Rigobello, S. Notarnicola, G. Magnifico, and S. Montangero, Phys. Rev. D **104**, 114501 (2021).
 - [12] M. Dalmonte and S. Montangero, Contemporary Physics **57**, 388 (2016), <https://doi.org/10.1080/00107514.2016.1151199>.
 - [13] P. Arrighi, C. Bény, and T. Farrelly, Quantum Information Processing **19** (2020), 10.1007/s11128-019-2555-4.
 - [14] L. Piroli and J. Cirac, Physical Review Letters **125** (2020), 10.1103/physrevlett.125.190402.
 - [15] K. Sellapillay, P. Arrighi, and G. D. Molfetta, “A discrete relativistic spacetime formalism for 1+1-qed with continuum limits,” (2022), arXiv:2103.13150 [quant-ph].
 - [16] T. A. Brun and L. Mlodinow, Entropy **27**, 492 (2025), arXiv:2503.05998 [quant-ph].
 - [17] G. Magnifico, D. Vodola, E. Ercolessi, S. P. Kumar, M. Müller, and A. Bermudez, Phys. Rev. B **100**, 115152 (2019).
 - [18] F. M. Surace, P. P. Mazza, G. Giudici, A. Leroze, A. Gambassi, and M. Dalmonte, Phys. Rev. X **10**, 021041 (2020).
 - [19] N. Klco, E. F. Dumitrescu, A. J. McCaskey, T. D. Morris, R. C. Pooser, M. Sanz, E. Solano, P. Lougovski, and M. J. Savage, Phys. Rev. A **98**, 032331 (2018).
 - [20] E. A. Martinez, C. A. Muschik, P. Schindler, D. Nigg, A. Erhard, M. Heyl, P. Hauke, M. Dalmonte, T. Monz, P. Zoller, and R. Blatt, Nature **534**, 516 (2016).
 - [21] D. Banerjee, M. Dalmonte, M. Müller, E. Rico, P. Stebler, U.-J. Wiese, and P. Zoller, Phys. Rev. Lett. **109**, 175302 (2012).
 - [22] E. Zohar, J. I. Cirac, and B. Reznik, Phys. Rev. A **88**, 023617 (2013).

- [23] E. Zohar, J. I. Cirac, and B. Reznik, Phys. Rev. Lett. **109**, 125302 (2012).
- [24] E. Kapit and E. Mueller, Phys. Rev. A **83**, 033625 (2011).
- [25] L. Susskind, Phys. Rev. D **16**, 3031 (1977).
- [26] K. G. Wilson, Phys. Rev. D **10**, 2445 (1974).
- [27] K. G. Wilson, in *13th International School of Subnuclear Physics* (1975).
- [28] H. S. Sharatchandra, H. J. Thun, and P. Weisz, Nuclear Physics B **192**, 205 (1981).
- [29] P. H. Ginsparg and K. G. Wilson, Phys. Rev. D **25**, 2649 (1982).
- [30] D. B. Kaplan, Phys. Lett. B **288**, 342 (1992).
- [31] Y. Shamir, Nucl. Phys. B **406**, 90 (1993).
- [32] H. B. Nielsen and M. Ninomiya, Phys. Lett. B **105**, 219 (1981).
- [33] H. B. Nielsen and M. Ninomiya, Nuclear Physics B **185**, 20 (1981).
- [34] H. B. Nielsen and M. Ninomiya, Nuclear Physics B **193**, 173 (1981).
- [35] D. Friedan, Commun. Math. Phys. **85**, 481 (1982).
- [36] M. Goldhaber, L. Grodzins, and A. W. Sunyar, Phys. Rev. **109**, 1015 (1958).
- [37] R. P. Feynman and M. Gell-Mann, Phys. Rev. **109**, 193 (1958).
- [38] E. C. G. Sudarshan and R. E. Marshak, Phys. Rev. **109**, 1860 (1958).
- [39] D. Bakircioglu, P. Arnault, and P. Arrighi, “Fermion doubling in quantum cellular automata,” (2025), arXiv:2505.07900 [quant-ph].
- [40] X.-L. Qi and S.-C. Zhang, Reviews of Modern Physics **83**, 1057 (2011).
- [41] M. König, H. Buhmann, L. W. Molenkamp, T. Hughes, C.-X. Liu, X.-L. Qi, and S.-C. Zhang, Journal of the Physical Society of Japan **77**, 031007 (2008).
- [42] B. A. Bernevig, T. L. Hughes, and S.-C. Zhang, Science **314**, 1757 (2006).
- [43] B. A. Bernevig and T. L. Hughes, *Topological Insulators and Topological Superconductors* (Princeton University Press, 2013).
- [44] S.-Q. Shen, *Topological Insulators*, 2nd ed., Springer Series in Solid-State Sciences (Springer, Singapore, 2017).
- [45] J. Kogut and L. Susskind, Phys. Rev. D **11**, 395 (1975).
- [46] M. F. Atiyah and I. M. Singer, Bull. Amer. Math. Soc. **69**, 422 (1963).
- [47] T. Eguchi, P. B. Gilkey, and A. J. Hanson, Phys. Rept. **66**, 213 (1980).
- [48] For instance, left-handed fermions carry nonzero weak isospin, whereas right-handed fermions are isospin singlets.
- [49] C. L. Kane and E. J. Mele, Physical Review Letters **95** (2005), 10.1103/physrevlett.95.146802.
- [50] R. Jackiw and C. Rebbi, Phys. Rev. D **13**, 3398 (1976).
- [51] J. Smit, *Introduction to Quantum Fields on a Lattice*, Cambridge Lecture Notes in Physics (Cambridge University Press, 2002).
- [52] C. G. Callan and J. A. Harvey, Nucl. Phys. B **250**, 427 (1985).

Appendix A: Derivation of the Fermionic Correlators

We derive the equal-time ground-state correlators used in Sec. V. The calculation proceeds in three steps: (A.1) free theory without chirality; (A.2) the gauged extension and gauge-independence; (A.3) the full chiral case.

A.1 Free theory

We work with the free flavoured Hamiltonian ($A_n = 0$), labelling unit cells by m (even site $n = 2m$, odd site $n+1 = 2m+1$). For a single chirality $\sigma = +$ the relevant hopping term is

$$H_f^+ = \frac{i}{2a} \sum_m [(\chi_{2m}^+)^\dagger (\psi_{2m+1}^+ - \psi_{2m-1}^+)] + \text{h.c.} \quad (\text{A1})$$

The unit cell has size $2a$, so the BZ is $k \in [-\pi/2a, \pi/2a]$. Expanding in Fourier modes,

$$\chi_{2m}^+ = \sqrt{\frac{2}{N}} \sum_k e^{i(2m)ka} c_k^+, \quad \psi_{2m+1}^+ = \sqrt{\frac{2}{N}} \sum_k e^{i(2m+1)ka} d_k^+, \quad (\text{A2})$$

where c_k^\pm, d_k^\pm satisfy canonical anti-commutation relations. Substituting,

$$H_f^+ = -\frac{1}{a} \sum_k \sin(ka) (c_k^{+\dagger} d_k^+ + d_k^{+\dagger} c_k^+). \quad (\text{A3})$$

At each k the 2×2 single-particle matrix has eigenvalues $\pm |\sin(ka)|/a$. The lower-energy (filled) mode and its expectation value are

$$\alpha_k^+ = \frac{c_k^+ + \text{sgn}(\sin ka) d_k^+}{\sqrt{2}}, \quad \langle c_k^{+\dagger} d_k^+ \rangle = \frac{1}{2} \text{sgn}(\sin ka). \quad (\text{A4})$$

By translational invariance the real-space correlator is site-independent:

$$\langle (\chi_n^+)^\dagger \psi_{n+1}^+ \rangle \xrightarrow{N \rightarrow \infty} \frac{1}{2\pi} \int_{-\pi/2}^{\pi/2} e^{iu} \text{sgn}(\sin u) du, \quad (\text{A5})$$

where $u = ka$. Since $\text{sgn}(\sin u) = \text{sgn}(u)$ for $u \in (-\pi/2, \pi/2)$:

$$\begin{aligned} \langle (\chi_n^+)^\dagger \psi_{n+1}^+ \rangle &= \frac{1}{2\pi} \left[\int_0^{\pi/2} e^{iu} du - \int_{-\pi/2}^0 e^{iu} du \right] \\ &= \frac{1}{2\pi i} [(e^{i\pi/2} - 1) - (1 - e^{-i\pi/2})] = \frac{i}{\pi}. \end{aligned} \quad (\text{A6})$$

Since $(\chi_n^+)^\dagger \psi_{n+1}^+ - (\psi_{n+1}^+)^\dagger \chi_n^+$ is anti-Hermitian, $\langle (\psi_{n+1}^+)^\dagger \chi_n^+ \rangle = -i/\pi$, and

$$\langle (\chi_n^+)^\dagger \psi_{n+1}^+ - (\psi_{n+1}^+)^\dagger \chi_n^+ \rangle = \frac{2i}{\pi}. \quad (\text{A7})$$

A.2 Gauged theory: gauge-independence

For the gauged Hamiltonian H_{sch}^f with a uniform $U(1)$ background $\forall U_n = e^{i\theta}$, $\theta = gAa$ on all links, the Fourier analysis of Eq. (A3) goes through with the replacement $e^{\pm ika} \rightarrow e^{\pm i(ka-\theta)}$, giving

$$H_{\text{sch}}^{f,+} |_{U_n=e^{i\theta}} = -\frac{1}{a} \sum_k \sin(ka - \theta) (c_k^{+\dagger} d_k^+ + d_k^{+\dagger} c_k^+). \quad (\text{A8})$$

The dispersion is shifted $k \rightarrow k - \theta/a$, and the gauge-invariant correlator evaluates to

$$\langle (\chi_n^+)^\dagger U_n^\dagger \psi_{n+1}^+ \rangle = \frac{e^{-i\theta}}{2\pi} \int_{-\pi/2}^{\pi/2} e^{iu} \text{sgn}(\sin(u - \theta)) du. \quad (\text{A9})$$

Substituting $v = u - \theta$ and splitting at $v = 0$ (which lies inside the integration range for $|\theta| < \pi/2$):

$$\langle (\chi_n^+)^\dagger U_n^\dagger \psi_{n+1}^+ \rangle = \frac{1}{2\pi i} \left[e^{-i\theta} \underbrace{(e^{i\pi/2} + e^{-i\pi/2})}_{=0} - 2 \right] = \frac{i}{\pi}. \quad (\text{A10})$$

The result is independent of θ . This is not accidental: in one spatial dimension there are no gauge-invariant plaquettes, the gauge field is pure gauge, and one can

always reach the axial gauge $U_n = 1$ by a local transformation [45, 51]. Hence the gauge-invariant observable $\langle (\chi_n^+)^\dagger U_n^\dagger \psi_{n+1}^+ - (\psi_{n+1}^+)^\dagger U_n \chi_n^+ \rangle$ must equal its free-theory value:

$$\langle (\chi_n^+)^\dagger U_n^\dagger \psi_{n+1}^+ - (\psi_{n+1}^+)^\dagger U_n \chi_n^+ \rangle = \frac{2i}{\pi}. \quad (\text{A11})$$

A.3 Including chirality

For $\sigma = -$ the Hamiltonian carries a global sign flip relative to $\sigma = +$:

$$H_f^- = -\frac{i}{2a} \sum_m [(\chi_{2m}^-)^\dagger (\psi_{2m+1}^- - \psi_{2m-1}^-)] + \text{h.c.}, \quad (\text{A12})$$

giving in momentum space $H_f^- = +(1/a) \sum_k \sin(ka) (c_k^{-\dagger} d_k^- + \text{h.c.})$. The sign flip swaps which linear combination is the lower-energy mode:

$$\langle c_k^{-\dagger} d_k^- \rangle = -\frac{1}{2} \text{sgn}(\sin ka). \quad (\text{A13})$$

The BZ integral then picks up a global minus sign, giving $\langle (\chi_n^-)^\dagger \psi_{n+1}^- \rangle = -i/\pi$. Collecting both chiralities, and noting that the gauge-independence argument of Sec. A.2 applies unchanged for $\sigma = -$:

$$\langle (\chi_n^\pm)^\dagger U_n^\dagger \psi_{n+1}^\pm - (\psi_{n+1}^\pm)^\dagger U_n \chi_n^\pm \rangle = \pm \frac{2i}{\pi}. \quad (\text{A14})$$

This result is purely imaginary (as required by anti-Hermiticity), independent of the lattice site n (translational invariance), and independent of the gauge background (1+1D pure gauge). It is the key input to the chiral anomaly calculation in Sec. V.